

Effect of Wind Shear Coefficients on Electrical Energy Generation in Lunga, Zambia

Sydney Mutale^{ab*}, Yong Wang^a, Jan Yasir^{ac}, Aboubacar Traore^a and Mamadou Suoare^a

^aSchool of New Energy, North China Electric Power University, Changping, Beijing, PR China

^bSchool of Engineering, University of Zambia, Lusaka, Zambia

^cBalochistan Residential College Turbat, Ministry of Education, Balochistan, Pakistan

Corresponding Author

Sydney Mutale, School of New Energy, North China Electric Power University, Changping, Beijing, PR China.

Submitted: 2024 Aug 07; Accepted: 2024 Aug 19; Published: 2024 Sep 02

Citation: Mutale, S., Wang, Y., Yasir, J., Traore, A., Suoare, M. et al. (2024). Effect of Wind Shear Coefficients on Electrical Energy Generation in Lunga, Zambia. *Earth Envi Scie Res & Rev*, 7(3), 01-12.

Abstract

Wind measurements are usually conducted at lower heights due to economic constraints and, after that, extrapolated to higher heights to estimate the wind speed. In order to understand the effects of wind shear coefficients on electrical energy on the Lunga site, the values were taken using 10-minute wind speed data measured at 40, 50, and 60 meters above ground level. If a constant value of the wind shear coefficient is used, the actual and extrapolated wind speed measurements will significantly differ. The resulting errors will affect the energy yield analysis (EYA) of the wind turbines. Vergnet 0.2 MW and Vestas 3.45 MW wind turbine power curves were used to analyze the effect of wind shear coefficient from March 2017 to August 2021. Air temperature and surface pressure data were used to calculate the wind power density. Further, the study's mean air density was 1.108 kg/m³, and the mean wind shear coefficient calculated for the Lunga site was 0.246. The results of EYA for the two turbines show higher variation and uncertainty in electrical energy generated at lower heights than at higher heights due to higher wind shear coefficients at lower heights. The results of 0.143 power law and the actual wind shear coefficient results above ground level showed increased EYA and capacity factor for higher heights than lower heights. These findings will be important as guidance for analyzing the effects of wind shear coefficients on electrical energy generation in Zambia.

Keywords: Wind Shear, Electrical Energy, Wind Turbine and Wind Power Density

1. Introduction

There are only three notable wind resource assessment studies in Zambia [1-5]. These are the renewable energy wind mapping program for Zambia (ESMAP), which analyzed wind characteristics at 20 m, 40 m, 60 m, and 80 m RINA on behalf of Kafue Gorge Regional Training Centre (KGRTC) at 60 m and Technology Development and Advisory Unit (TDAU), University of Zambia at 40 m, 50m and 60 m [3,4]. The estimated energy production based on a generic 4 MW wind turbine with a rotor of 140 m and a hub height of 130 m for ESMAP was after extrapolation [1].

The RINA at KGRTC was for training applications; no further extrapolation was done to understand wind characteristics at higher heights. The extrapolation by TDAU was at a hub height of 116.5 m. In addition to the three studies, various studies have been conducted to contribute to the growth of the renewable energy

sector in Zambia [4,6-8]. It is essential to understand the effects of wind shear on lower and higher heights. Wind shear is a change in wind speed or direction over a short distance. It is usually measured horizontally or vertically and associated with strong temperature inversions or density gradients. It is known that a 1% error in the measurement of wind speed translates into an error of almost 2% in energy production (Rehman et al.,). Abbreviations: WSC, Wind Shear Coefficient; EYA, Energy Yield Analysis; AEP, Annual Energy Production; AF, Availability Factor; CF, Capacity Factor; Stdv, Standard Deviation; FLH, Full Load Hour; AEY, Annual Energy Yield; AEP, Annual Energy Production; MW, Mega Watt; P, Wind Power (W); W/m², Watt Per Meter Square; P (V), Wind Turbine's Power Curve; C, Weibull Scale Parameter; K, Weibull Shape Parameter; ln, Natural Logarithm; MWh, MegaWatt hour; h/yr, hour Per Year; K, Kelvin; KWh, Kilo Watt-hour; J/Kg, Joule per Kilogram; v, Wind Velocity (m/s); ρ, Air density [4].

Wind shear occurs typically at high or low altitudes. It is a micro-scale weather phenomenon that occurs over a minimal distance, but it can be associated with mesoscale or brief weather features such as squalls and cold fronts. It is associated with microbursts and squalls caused by thunderstorms, stronger deep winds near mountains, weather fronts, radiation swings, calm winds, buildings, wind turbines, sailboats, and observed boats. Accurate assessment of wind resources is a crucial factor that must be fully understood to harness wind power (Rehman et al., 2022; In order to accurately characterize the vertical wind speed profile, there is need to explore the use of remote sensing for site prospecting in Zambia [4,9].

The known power factor of 1/7 power law is used to extrapolate wind to a particular hub height. This coefficient depends on where the measurements are made, and if the wind shear coefficient is greater than 1/7, the power law leads to an underestimation of the wind speed (Rehman et al., 2022). The wind speed at a given height increases by a power factor called wind shear factor or wind shear coefficient with altitude. Therefore, it is vital to understand the wind shear coefficient, which is fundamental for estimating wind power. Air density is another critical parameter that directly affects power generation measurements and wind speed because it depends on the temperature and surface pressure of a selected location. For this reason, an assumed value of air density will affect energy production by underestimating or overestimating. In order to avoid affecting energy production, each location's air density must be determined using the location's pressure measurements and temperature to allow for an accurate energy estimation.

In most of the data collection stations in the world, wind speed is measured at only one specific height, due to which wind shear values are hardly available [10]. Several studies have focused on the examination of wind shear and atmospheric conditions to analyze stable, unstable, and neutral states of stability due to thermal factors in diurnal variation, which influences the production of energy; differences may result in errors in the annual energy production (AEP) calculation [11]. The study conducted by Okorie et al. in southern Namibia showed that the hub height and energy yield were dependent on the wind shear coefficient, and the mean wind shear coefficient was 0.197 and 0.132, with the minimum in summer and maximum values in winter. The diurnal values were maximum at night and minimum in daylight hours. In Jeju Island, South Korea, analyzed atmospheric factors, stability, and wind shear exponent on the wind power performance and annual energy production [7,12].

(AEP) of wind turbines; it was found that there was a variation of 1.4-4% due to a difference in Wind shear exponent analyzed wind shear and its effects on annual energy production for Phagan Island collected at 65m and 120m above ground level with the help of Weibull parameters, which showed up to 35% difference in Wind energy production due to variation in wind shear coefficient. Measured wind shear coefficient variability at three coastal sites of Malaysia at a height of 55m to 70m from ground level by using

the Power law equation. Wind shear values larger than the power law (0.143) were observed, which confirms the variation in wind energy potential with the change in wind shear coefficient [13,14].

In the study by one-year wind data was collected in Balikesir using power law and Weibull parameters to show the effect of wind shear coefficient on energy production. The difference in wind energy production from data at hub height and extrapolated data was up to 49.6% due to wind shear coefficient influence. calculated the wind shear coefficient for three coastal locations in southern Italy by using power law for diurnal, monthly, and annual variation. The study also analyzed the energy yield of extrapolated data at 50m from 10m using wind roses, wind speed frequency distribution, and Weibull's parameters. (Rehman et al., 2022) in Dhahran, Saudi Arabia, analyzed the data at 20 m, 30 m, and 40m to assess the effect of wind shear coefficient on energy yield from a wind farm of 60MW. It was observed that higher values of wind shear coefficient occurred during nighttime and were smaller in daylight hours [11,15].

The energy yield achieved was around 11-12% more for the actual wind shear coefficient compared with the one obtained using the 1/7 power law. analyzed the effect of diurnal wind shear and found that the maximum was at nighttime and a minimum during the day; this suggests cooling of the ground surface and air above it. calculated annual mean wind shear on 2-year data in Hungary with elevation of 20m and 50m above ground level and found the value of wind shear between 0.45-0.50. This study analyzes the effect of wind shear coefficients on electrical energy generation in Lunga District, using wind speed data collected using RNRG Systems 60 m XHD tall tower met mast at 40 m, 50 m, and 60 m taking into consideration the variability of vertical and horizontal wind speeds, the power performance of different suitable turbines was analyzed. The temperature and pressure measurements of the site were used to calculate the air density [4,10,14].

The study analyzes the effect of wind shear on the distribution and measurements of the differences in the power curve (Table 1) and annual energy production with the variation in atmospheric factors.

2. Materials and Methods

2.1. Site Description

Lunga District is located on the banks of Lake Bangweulu in the swampy area shown in Fig. 1. The location (Fig. 2) where the mast is installed is at coordinates 11°25'0.60" S and 30° 9'13.80"E approximately 2km east of the Rural Electrification (REA) solar power plant and across the lake channel which is used as water transport route. The average annual temperature is about 25.5 degrees Celsius, with an average of 98.2 mm of rainfall. The site is located within the land that is used for both residential and agricultural activities east of the Zambia Information and Telecommunication Agency (ZICTA) tower, approximately 1km. The topography of the site is flat and seasonally waterlogged; however, the area characteristics change away from the channel. The land is under customary ownership, and the use of this land

for wind power generation will require the chiefs involvement and sensitization for the current users. People in the area have limited sources of energy because there is limited firewood and no electricity. People collect firewood from the mainland for heating

and cooking through water channels using boats and canoes. There is a need to explore wind energy as an alternative source for the local people and Institutions for lighting, heating, and cooking.



Figure 1: Project site in Lunga District

Fig. 2 shows the tower measuring wind speed at 40 m, 50 m, and 60 m in Lunga District.



Figure 2: Mast

2.2. Method

To understand the variation of the wind shear coefficient for the site, diurnal, seasonal, monthly periods, and Weibull parameters were considered. The methodology used involved assigning two suitable turbines for the sites, Vergnet 0.2 MW and Vestas 3.45 MW, with power curves shown in Table 1, then comparing the data measured with the actual site calculated wind shear coefficient and those calculated using 0.143 power law as follows:

- Applying $\alpha = 0.143$ for data extrapolation from 40 m.
- Applying the calculated mean wind shear coefficient for the site.
- Comparing the measured data at 60 m and extrapolated heights of 120 m

The results were obtained by numerical calculations and compared with WAsP software results for EYA analysis using the formulas in the next section.

Vergnet 0.2 MW			Vestas 3.45 MW		
Wind Speed [m/s]	Power [kW]	Thrust coefficient (C_T)	Wind speed [m/s]	Power [kW]	Thrust coefficient (C_T)
4.0	3.0	0.11	2	-	-
4.5	8.0	0.20	3	22	0.87
5.0	14.0	0.26	4	150	0.83
5.5	21.0	0.29	5	340	0.83
6.0	29.0	0.31	6	617	0.82
6.5	40.0	0.34	7	1,006	0.82
7.0	53.0	0.36	8	1,522	0.79
7.5	67.0	0.37	9	2,178	0.79
8.0	82.0	0.37	10	2,905	0.73
8.5	98.0	0.37	11	3,374	0.58
9.0	116.0	0.37	12	3,448	0.42
9.5	135.0	0.36	13	3,450	0.32
10.0	154.0	0.35	14	3,450	0.25
10.5	176.0	0.35	15	3,450	0.20
11.0	190.0	0.33	16	3,450	0.16
11.5	198.0	0.30	17	3,450	0.14
12.0	200.0	0.27	18	3,450	0.12
12.5	200.0	0.24	19	3,450	0.10
13.0-25.0	200.0	0.21-0.5	20	3,450	0.09

Table 1: Vergnet 0.2 MW and Vestas 3.45 MW with power curves

3. Vertical Extrapolation of Mean Wind Speed

Various mathematical models are used to describe the vertical profile of wind speed. The logarithmic law calculates the average wind speed V at height Z . This method depends on the roughness Z_0 in the situation of neutral stability. For a relatively flat field close to the ground, the calculation is as shown in the following equation:

$$\frac{V_1}{V_0} = \left(\frac{Z_1}{Z_0}\right)^\alpha \quad (1)$$

Where α is a coefficient, i.e., the Hellmann exponent varies between 0.1 and 0.4, dependent on the roughness of the terrain [4,13,15,16]. The exponent is highly dependent and can be expressed as:

$$\alpha = \frac{\ln(v_2/v_1)}{\ln(h_2/h_1)} \quad (2)$$

4. Wind Analysis Model

To calculate the frequency distribution of wind speeds, WAsP uses the Weibull function shown in the following equation:

$$f(v) = \left(\frac{k}{c}\right) \left(\frac{v}{c}\right)^{k-1} \exp\left(-\frac{v}{c}\right)^k \quad (3)$$

Here c is the scale parameter while k is the shape factor. Several

numerical methods can be used for Weibull parameters estimation (Gaddada et al., 2016). The corresponding cumulative distribution function is shown in the equation below:

$$F(v) = 1 - \exp\left[-\left(\frac{v}{A}\right)^k\right] \quad (v > 0; k, A > 0) \quad (4)$$

5. Air Density

Air density is one of the critical parameters when calculating wind energy profile from a site, as it is directly proportional to power density. It depends on ambient air temperature and atmospheric pressure and may be calculated using Eq. 4, reported by (Adnan et al., 2021):

$$\rho = \frac{p}{RT} \quad (5)$$

5.1. Wind Power Density

The power of the wind that flows at a speed of (v) through a blade sweep area of (S_w) is as shown in the equation below;

$$P(v) = \frac{1}{2} S_w \rho v^3 \quad (6)$$

Where ρ is the air density, it is well known that the power of the wind that flows at speed v through a blade sweep area A increases as the cubic of its velocity [13,14,17]. The calculation of the wind power density of a site based on a Weibull probability density function is as shown in the following equation (Fazelpour et al.,2017):

$$\frac{P}{S_w} = \frac{1}{2} \rho A^3 \Gamma \left(1 + \frac{3}{k} \right) \quad (7)$$

6. Results and Discussions

6.1. Wind Data Characteristics

Wind data was analyzed using data recordings from March 2017 to August 2021 and quarterly to understand the seasonal variations at 40 m, 50 m, and 60 m. The tower has two anemometers at 40 m, 50 m, and 60 m for left and right orientation, a wind vane at 57.5 m for right orientation, a 1 wind vane at 47.5 m for left orientation,

four thermometers, and four barometers. The graphs and tables were grouped into categories, namely, wind speed distribution, cumulative daily wind speed averages, wind rose, and cumulative daily pressure distribution for the report period. The data presented below is from March 2017 to August 2021. This period is the rainy season, and the characteristics differ from the other seasons.

Fig. 3, Fig. 4 and Fig. 5. show the wind speed frequency distribution at 60m,50m, and 40m. The wind distribution at the three levels has shown normal behavior, as indicated by the distribution curves fitted to the graphs.

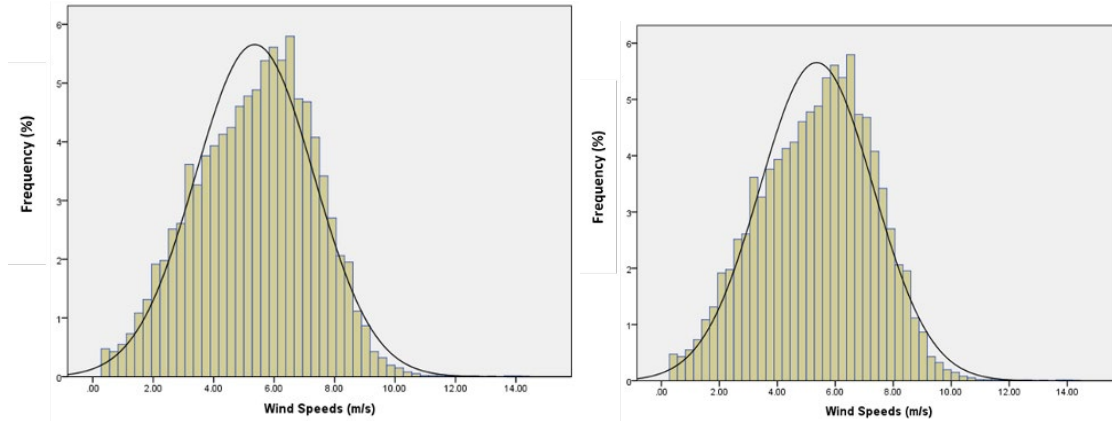


Figure 3: Anemometer 60R and 60L

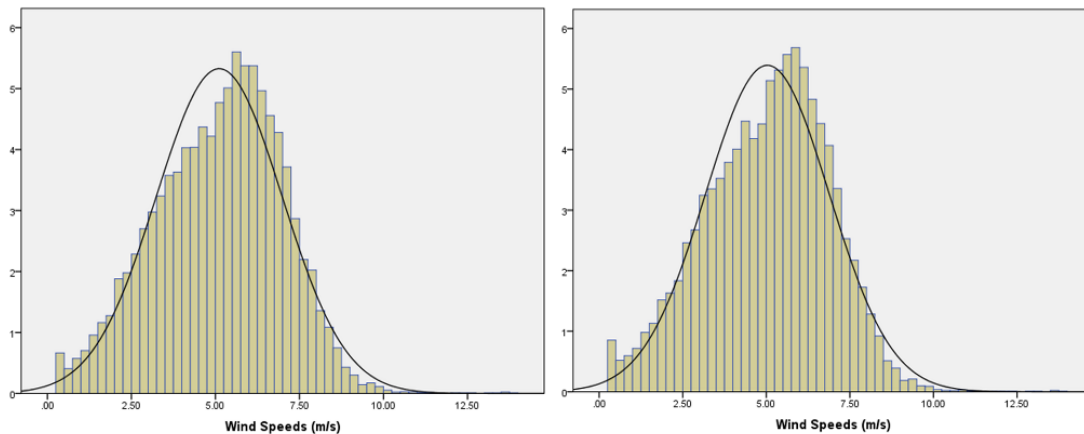


Figure 4: Anemometer 50R and 50L

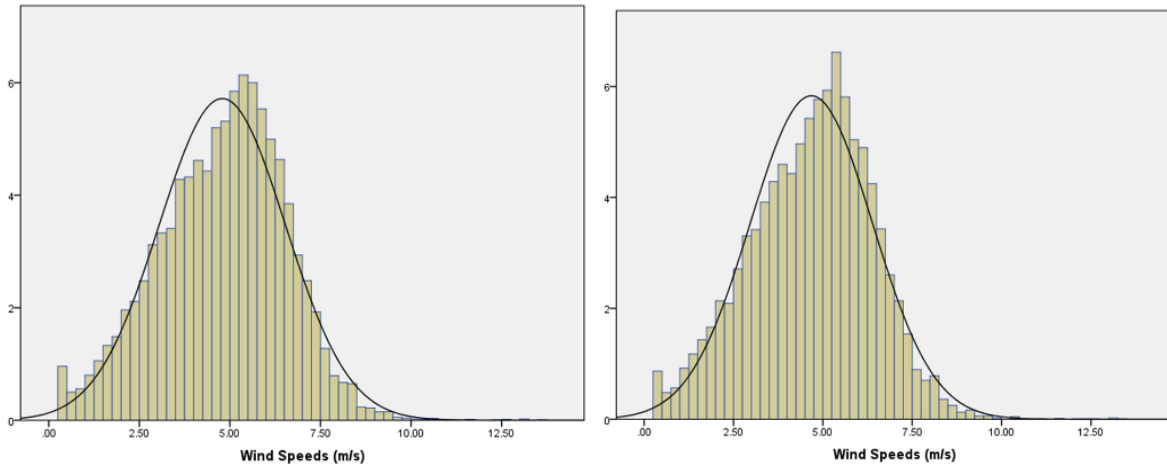


Figure 5: Anemometer 40R and 40L

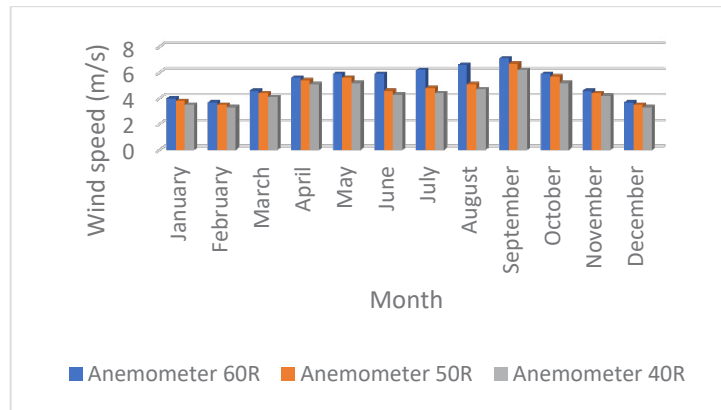


Figure 6: Anemometer monthly average wind speed comparison 60R, 50R and 40R

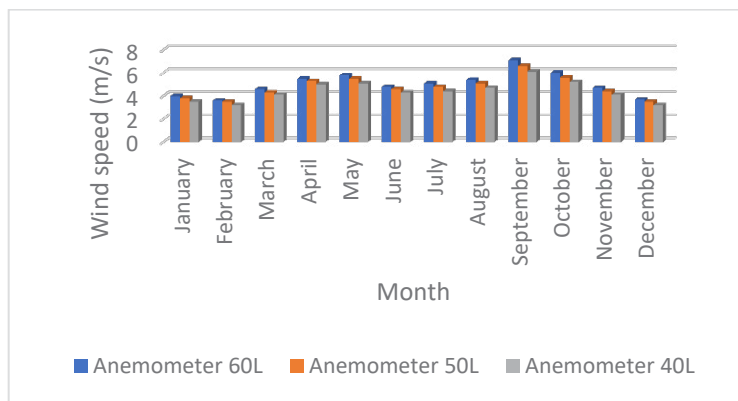


Figure 7: Anemometer monthly average wind speed comparison 60L, 50L and 40L

Fig. 8 and Fig. 9. show the wind speed frequency distribution at 40m,50m, and 60m. The wind distribution at the three levels has shown normal behavior, as indicated by the distribution curves fitted to the graphs.

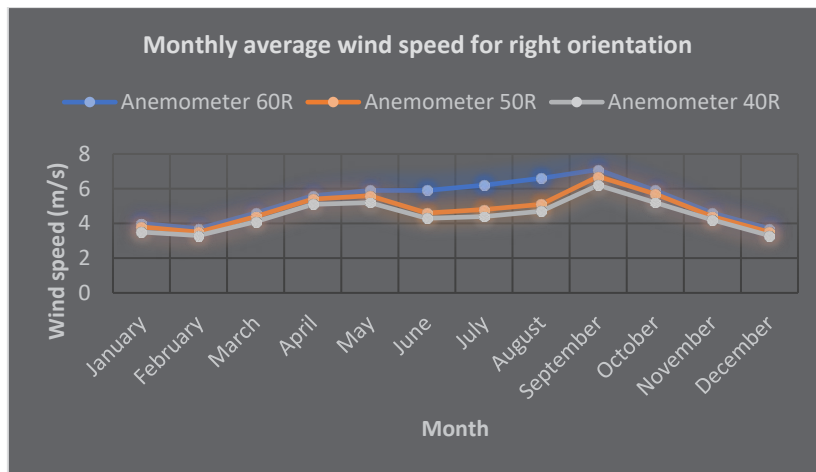


Figure 8: Monthly average wind speed right orientation

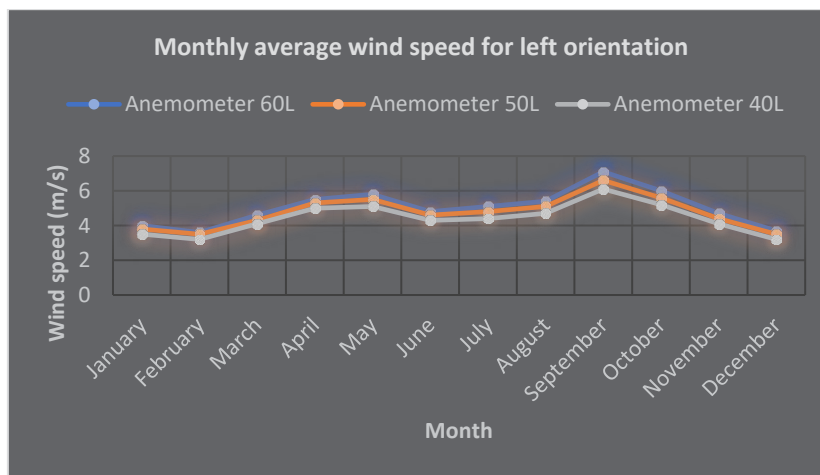


Figure 9: Monthly average wind speed for left orientation

The two daily mean wind speed graphs presented in Fig. 10 and Fig. 11 indicate that higher wind speeds are during the night-time hours between 20 hours to 23 hours. The lower winds are during daylight hours between 13 hours to 16 hours.

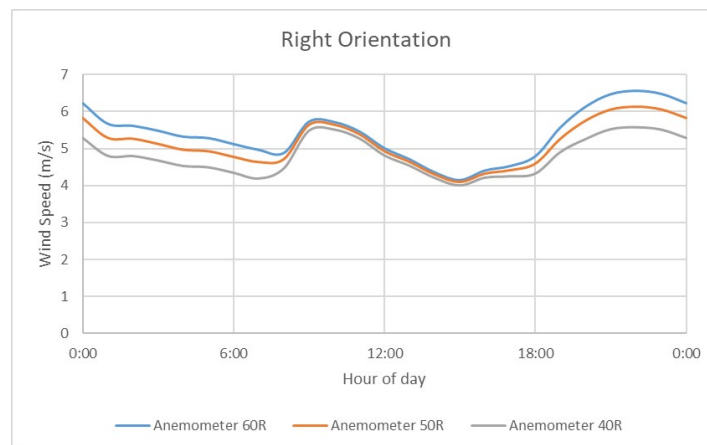


Figure 10: Diurnal behaviour for right and left orientation

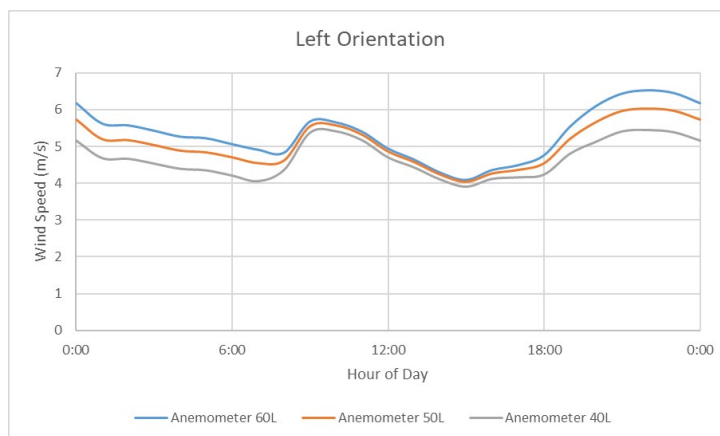


Figure 11: Diurnal behaviour for right and left orientation

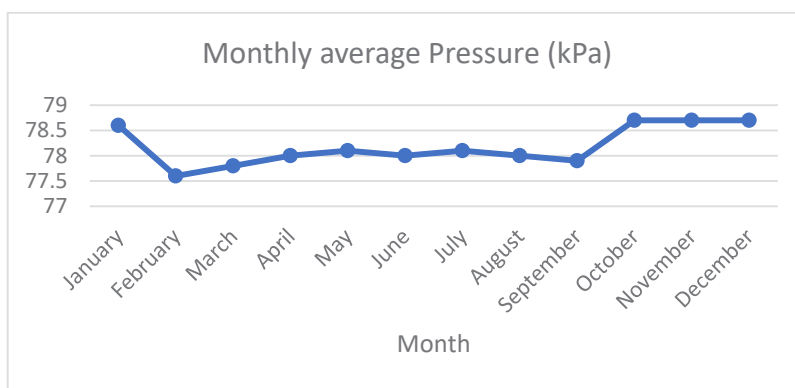


Figure 12: Average daily pressure

The cumulative wind speed average graphs shows the behaviour of the daily wind speed average over the report period. The monthly wind speed averages for the right orientation was reported

at 5.4m/s, 5.1m/s and 4.8m/s respectively. Whereas the Left orientation averages was found to be 5.3m/s, 5.0m/s and 4.7m/s respectively. Fig. 12 shows the average daily pressure.

Month	Anemometer 60R/60L (m/s)		Anemometer 50R/50L (m/s)		Anemometer 40R/40L (m/s)		Average Pressure (kPa)
January	4.0	4.0	3.8	3.8	3.5	3.5	78.6
February	3.7	3.6	3.5	3.5	3.3	3.2	77.6
March	4.6	4.6	4.4	4.3	4.1	4.1	77.8
April	5.6	5.5	5.4	5.3	5.1	5.0	78.0
May	5.9	5.8	5.6	5.5	5.2	5.1	78.1
June	5.9	4.8	4.6	4.6	4.3	4.3	78.0
July	6.2	5.1	4.8	4.8	4.4	4.4	78.1
August	6.6	5.4	5.1	5.1	4.7	4.7	78.0
September	7.1	7.1	6.7	6.6	6.2	6.1	77.9
October	5.9	6.0	5.7	5.6	5.2	5.2	78.7
November	4.6	4.7	4.4	4.4	4.2	4.1	78.7
December	3.7	3.7	3.5	3.5	3.3	3.2	78.7

Table 2: Wind speed, energy yield parameters for the Lunga site

7. Air Density Analysis

The monthly mean air density values shown in Table 2 are higher in the cold season, May, June, and July, with June having the highest of 1.257 kg/m³. The lowest values are in the hot season: September, October, and November, with October being the hottest month in the country, having the lowest at 0.894 kg/m³. In the rainy season, which spans from December to April, January has the highest value of 1.172 kg/m³ in the rain season however,

the change is negligible. The overall mean density for the site ranges from 0.894 kg/m³ to 1.257 kg/m³. The coldest month of June has an air density of 1.223, which is close to the real value of air density of 1.225 kg/m³. This data is backed by literature (Rehman et al., 2007) about air density for June [10]. Therefore, energy yield is likely higher during the cold season, followed by the rainy season, and lowest in the hot season for the site.

Month	Air density(kg/m ³)	Wind shear coefficient
January	1.172	0.13
February	1.140	0.14
March	1.147	0.11
April	1.167	0.09
May	1.194	0.13
June	1.257	0.61
July	1.223	0.63
August	1.059	0.64
September	0.928	0.14
October	0.894	0.09
November	0.984	0.11
December	1.131	0.14

Table 3: Air density and Wind shear coefficient for Lunga

The data measured at 10 minutes from 40 m to 60 m using equation 2, the annual wind shear ground level using 60 m right and left 50 m right and left, and 40 m right and left orientation.

It was observed that wind shear generally varies with height and is constant at minimal height differences. Fig. 13 shows the wind shear coefficient annual variation.

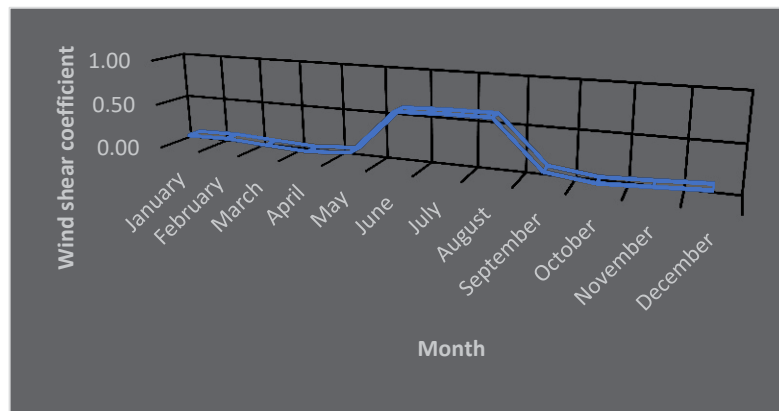


Figure 13: Wind shear coefficient annual variation

As shown in Fig. 13, the wind shear coefficient values are higher in the cold season with the range of 0.61- 0.64, while the hot and rainy seasons have the lowest values of wind shear coefficients ranging from 0.09-0.14. The mean wind shear coefficient calculated for the Lunga site was 0.246. There is higher air mixing in the hot season above the ground level and minimal air mixing in the cold season. Therefore, this may affect the energy yield in the hot and rainy seasons since the air density is at its lowest; this is consistent with studies conducted by references (Rehman et al., 2007; Ulazia

et al., 2019). This scenario is similar to the diurnal wind shear coefficient variation [10]. The study shows that higher values of wind shear coefficient were obtained during the night due to the daily heating and cooling cycle of the air, which occurs above the ground level. The values of wind shear coefficient start to decrease as the sun rises and start to heat the air near the ground level. It was observed that the values remain stable and start to increase when the sun intensity reduces around 17 hours as the air above the ground level starts cooling down. This results in a gradual turn

in the stable condition, as supported by reference.

8. Wind Energy Yields Analysis

From the analysis given in the previous sections, it is concluded that the wind shear coefficient plays a vital role in wind speed measurements for any height. Due to limited resources, several studies assess energy yields at higher heights by measuring wind

speeds at lower heights and then applying extrapolation methods. There are specific constant values that are used for different terrains. Table 4 shows wind shear coefficient values. Lunga sites are classified to fall between tall crops, hedges, and shrubs and small towns with some trees and shrubs, with the wind shear coefficient of 0.20 to 0.30, which is consistent with the mean value of wind shear coefficient calculated in this study of 0.246.

Terrain	Wind shear coefficient (α)
Lack, ocean and smooth hard ground	0.10
Foot high grass on level ground	0.15
Tall crops, hedges, and shrubs	0.20
Wooded country with many trees	0.25
Small towns with some trees and shrubs	0.30
City area with tall buildings	0.40

Table 4: Wind shear coefficient values for various terrains (Albani et al., 2021)

A slight change in wind shear can affect the wind speed at a certain height greatly (Mohamadi et al., 2021). Analyzing the data collected at 60 m for the Lunga site, using Vergnet 0.2 MW, the results are shown in Table 5. The mean wind speed at 60 m is 5.4 m/s and 261.71 W/m². The EYA for the Lunga site was calculated at 60 m using Vergnet 0.2 MW, showing a capacity factor (CF) of (15.0%) and an availability factor (AF) of (92.4%). Comparing the extrapolated data using $\alpha=0.143$ with 60 m measured data shows an underestimation of (5.6 %) of the mean wind speed results with 10.2 % for CF and AF 1.6 %. Further, comparing the extrapolated data using $\alpha=0.246$ shows an underestimation of (9.4 %) of the

mean wind speed results with 15.6 % for CF and AF 1.6 %. The results show that wind shear varies with height; lower values were calculated at higher altitudes and higher values at lower heights. The AEY calculated is also higher at 60 m because it has less wind shear coefficient results compared to the lower level of 40 m. The results of EYA for Vergnet 0.2 MW show higher variation and uncertainty in electrical energy generated at lower heights than at higher heights due to higher wind shear coefficients; this can be seen from the results of extrapolation from 40 m using $\alpha=0.143$ and the site value extrapolation from 40 m using $\alpha=0.246$ [18].

Parameter	Wind data		
	Measured at 60m	Extrapolated from 40 m using $\alpha=0.143$	Extrapolated from 40 m using $\alpha=0.246$
Wind Data			
No. of Valid Data	224882	224442	224442
Valid Data %	96.4	96.2	96.2
Mean	5.40	5.10	4.89
Stdv	1.12	1.06	1.01
C	6.50	6.16	5.84
K	1.26	1.20	1.14
Mean P (W/m ²)	261.71	220.47	194.34
Turbine Converted Energy			
AEY (MWh/yr)	525.0	471.45	371.70
CF (%)	15.00	13.47	10.62
FLH (h/yr)	1,276	1146	1077
AF (%)	92.4	90.80	88.80

Table 5: EYA for Lunga using Vergnet 0.2 MW

Analyzing the data collected at 60 m for the Lunga site, using Vestas 3.45 MW, the results are shown in Table 6. The mean wind speed at 60 m is 5.4 m/s and power density of 1020.65 W/m². The EYA for the Lunga site calculated at 60 m using Vestas 3.45 MW shows a capacity factor (CF) of (24.04%) and an availability factor (AF) of (83.20%). Comparing the extrapolated data using $\alpha=0.143$ with 60 m measured data shows an increase of (19.4 %) for the mean wind speed results with 15.1 % for CF and AF 7.8 %. Further, comparing the extrapolated data using $\alpha=0.246$.

shows an increase of (15.6 %) for the mean wind speed results

with 11.7 % for CF and AF 6.3 %. The results show that wind shear varies with height; lower values can be calculated at higher altitudes and higher values at lower heights. The AEY calculated is also higher at 120 m because it has less wind shear coefficient results compared to the lower level of 60 m. The results of EYA for Vestas 3.45 MW show higher variation and uncertainty in electrical energy generated at lower heights than at higher heights due to higher wind shear coefficients. This can be seen from the results of extrapolation from 60 m using $\alpha=0.143$ and the site value extrapolation from 60 m using $\alpha=0.246$.

Parameter	Wind data		
	Extrapolated to 120 m using $\alpha=0.143$	Extrapolated to 120 m using $\alpha=0.246$	Measured at 60m
Wind Data			
No. of Valid Data	224882	224882	224882
Valid Data %	96.4	96.4	96.4
Mean	6.70	6.40	5.40
Stdv	2.26	1.84	1.12
C	6.90	6.60	6.50
K	2.05	1.75	1.26
Mean P (W/m ²)	1699.17	1490.10	1020.65
Turbine Converted Energy			
AEY (MWh/y)	17847	16866	14546
CF (%)	29.5	27.23	24.04
FLH (h/yr)	2,577	2,577	2,577
AF (%)	90.2	88.80	83.20

Table 6: EYA for Lunga using Vestas 3.45 MW

Conclusions

This study analyses how wind shear coefficients affect electrical energy generation. Lower heights are used to measure wind speed due to economic constraints, and after that, extrapolated to higher heights to estimate the wind speed. Using the data collected at 20 m, 40 m, and 60 m above ground level from March 2017 to August 2021, the wind shear coefficient was analyzed. The results show that wind shear varies with height; lower values can be calculated at higher altitudes and higher values at lower heights. The highest air density values are in the cold season: May, June, and July, with June having the highest of 1.257 kg/m³. The lowest values are in the hot season: September, October, and November, with October being the hottest month in the country, having the lowest at 0.894 kg/m³. The overall mean density for the site ranges from 0.894 kg/m³ to 1.257 kg/m³. The coldest month of June has an air density of 1.223 kg/m³, which is close to the actual value of air density of 1.225 kg/m³. The mean wind shear coefficient calculated for the Lunga site was 0.246. The wind shear coefficient values are higher in the cold season with the range of 0.61- 0.64, while the hot and rainy seasons have the lowest values of wind shear coefficients ranging from 0.09-0.14. There is higher air mixing

in the hot season above the ground level and minimal air mixing in the cold season. The EYA for the Lunga site was calculated at 60 m using Vergnet 0.2 MW, showing a capacity factor (CF) of (15.0%) and an availability factor (AF) of (92.4%). Comparing the extrapolated data using $\alpha=0.143$ with 60 m measured data shows an underestimation of (5.6 %) of the mean wind speed results with 10.2 % for CF and AF 1.6 %. Further, comparing the extrapolated data using $\alpha=0.246$ shows an underestimation of (9.4 %) of the mean wind speed results with 15.6 % for CF and AF 1.6 %. The EYA for the Lunga site calculated at 60 m using Vestas 3.45 MW shows a capacity factor (CF) of (24.04%) and an availability factor (AF) of (83.20%). Comparing the extrapolated data using $\alpha=0.143$ with 60 m measured data shows an increase of (19.4 %) of the mean wind speed results with 15.1 % for CF and AF 7.8 %. Further, comparing the extrapolated data using $\alpha=0.246$ shows an increase of (15.6 %) of the mean wind speed results with 11.7 % for CF and AF 6.3 %. Future studies should focus on studying wind shear characteristic in areas which are not swampy like Lunga. In order to accurately characterize the vertical wind speed profile, there is need to explore the use of remote sensing for site prospecting in Zambia. EYA is affected by the wind shear coefficient; therefore,

this data is essential as guidance for analyzing wind shear for wind power in Zambia [19-23].

References

1. Renewable Energy Wind Mapping for Zambia 12-month Site Resource Report the World Bank. (2018).
2. Ministry of Energy, Department of Energy, Lusaka, Zambia. (2023, October).
3. Banda, A., Simukoko, L., & Mwenda, H. M. (2019). A review of wind resource potential for grid-scale power generation in Zambia. UNESCO 6th Africa Engineering Week and 4th Africa Engineering Conference, on the 18th–20th September.
4. Mutale, S., Banda, A., Wang, Y., & Yasir, J. (2023). Capability of Zambian Industries to Manufacture Grid-Scale Wind Turbine Blades and Towers.
5. Mutale, S., Wang, Y., Yasir, J., Banda, A., & Aboubacar, T. (2023). Economic feasibility of onshore wind energy potential for electricity generation in Zambia.
6. Kaoma, M., Gheewala, S. H. (2021). Sustainability performance of lignocellulosic biomass³⁹⁴ to-bioenergy supply chains for Rural Growth Centres in Zambia. *Sustainable Production and Consumption*, 28, 1343–1365.
7. Kim, D. Y., Kim, Y. H., & Kim, B. S. (2021). Changes in wind turbine power characteristics and annual energy production due to atmospheric stability, turbulence intensity, and wind shear. *Energy*, 214, 119051.
8. Mwanza, M., Mwansa, K., Bowa, C. K., Sumbwanyambe, M., Pretorius, J. H., & Ulgen, K. (2022, April). Techno-economic Analysis of Wind/PV Hybrid System for Sustainable and Clean Energy Production for Shang’ombo District of Zambia. In *International Symposium on Energy Management and Sustainability* (pp. 431-442). Cham: Springer International Publishing.
9. Kalumba, M., Dondeyne, S., Vanuytrecht, E., Nyirenda, E., & Van Orshoven, J. (2022). Functional evaluation of digital soil hydraulic property maps through comparison of simulated and remotely sensed maize canopy cover. *Land*, 11(5), 618.
10. Azad, A. Alam, M. M., Saha M. Wind shear coefficients and energy yield for Dhahran, Saudi Arabia, *Renew. Energy*, (2011)1–6.
11. Wharton, S., & Lundquist, J. K. (2012). Assessing atmospheric stability and its impacts on rotor-disk wind characteristics at an onshore wind farm. *Wind Energy*, 15(4), 525-546.
12. St Martin, C. M., Lundquist, J. K., Clifton, A., Poulos, G. S., & Schreck, S. J. (2016). Wind turbine power production and annual energy production depend on atmospheric stability and turbulence. *Wind Energy Science*, 1(2), 221-236.
13. Werapun, W., Tirawanichakul, Y., & Waewsak, J. (2017). Wind shear coefficients and their effect on energy production. *Energy Procedia*, 138, 1061-1066.
14. Adnan, M., Ahmad, J., Ali, S. F., & Imran, M. (2021). A techno-economic analysis for power generation through wind energy: A case study of Pakistan. *Energy Reports*, 7, 1424-1443.
15. Firtın, E., Güler, Ö., & Akdağ, S. A. (2011). Investigation of wind shear coefficients and their effect on electrical energy generation. *Applied Energy*, 88(11), 4097-4105.
16. Mohamadi, H., Saeedi, A., Firoozi, Z., Zangabadi, S. S., & Veisi, S. (2021). Assessment of wind energy potential and economic evaluation of four wind turbine models for the east of Iran. *Heliyon*, 7(6).
17. Ucar, A., & Balo, F. (2009). Evaluation of wind energy potential and electricity generation at six locations in Turkey. *Applied Energy*, 86(10), 1864-1872.
18. Jan, Y., Ahmed, S., Wang, Y., & Sydney, M. (2023). An Investigation of Wind Shear Coefficients and Their Impact on Electrical Energy Generation in Coastal Locations of Balochistan, Pakistan.
19. Albani, A., Ibrahim, M. Z., & Yong, K. H. (2019). Wind shear data at two different terrain types. *Data in brief*, 25, 104306.
20. Kaoma, M., & Gheewala, S. H. (2021). Evaluation of the enabling environment for the sustainable development of rural-based bioenergy systems in Zambia. *Energy Policy*, 154, 112337.
21. Kaoma, M., & Gheewala, S. H. (2021b). Techno-economic assessment of bioenergy options using crop and forest residues for non-electrified rural growth centres in Zambia. *Biomass and Bioenergy*, 145, 105944.
22. Okorie, M. E., Inambao, F., & Chiguvare, Z. (2017). Evaluation of wind shear coefficients, surface roughness and energy yields over inland locations in Namibia. *Procedia Manufacturing*, 7, 630-638.

Copyright: ©2024 Sydney Mutale, et al. This is an open-access article distributed under the terms of the Creative Commons Attribution License, which permits unrestricted use, distribution, and reproduction in any medium, provided the original author and source are credited.